Spatial correlation of a particle-hole pair with a repulsive isovector interaction

K. Hagino [1] and H. Sagawa[2,3]

[1]*Department of Physics, Kyoto University, Kyoto 606-8502, Japan*
[2]*RIKEN Nishina Center for Accelerator-Based Science, Wako 351-0198, Japan*
[3]*Center for Mathematics and Physics, University of Aizu, Aizu-Wakamatsu, Fukushima 965-8560, Japan*

We study the spatial correlation of a particle-hole pair in the isovector channel in ^{56}Co and ^{40}K nuclei. To this end, we employ the Hartree-Fock+Tamm-Dancoff approximation with the Skyrme interaction. We find a large concentration of the two-body density at positions where the neutron particle and the proton hole states locate on the opposite side to each other with respect to the core nucleus. This feature originates from a repulsive nature of the isovector residual interaction, which is in stark contrast to the dineutron correlation with an attractive pairing interaction between the valence neutrons discussed, e.g., in ^{11}Li and ^{6}He.

I. INTRODUCTION

It has been well recognized that the pairing correlation among valence neutrons plays a decisive role in the structure of weakly bound nuclei [1–5]. In particular, there have been several theoretical studies of a strong dineutron correlation [4,6–10], in which two neutrons attract each other and show a large probability of a two-body wave function with a small correlation angle in the coordinate space. A strong signature of the dineutron correlation has also been found experimentally in several weakly bound nuclei such as ^{11}Li and ^{6}He [11–13], and more recently in ^{19}B [14].

It would be an interesting question to ask what happens to the spatial correlation when the interaction is repulsive rather than attractive. This could be learned from atomic physics, in which the primary interaction among electrons is the Coulomb repulsion. It has been actually known that the anticorrelation, opposite to the dineutron correlation, exists in the spatial distribution of two electrons in, e.g., He atoms [15–17]. This anticorrelation is referred to as the Coulomb hole, in which the correlation angle between two electrons is almost 180° in the spatial distribution. The purpose of this paper is to address to what extent a similar correlation exists in nuclear systems.

Besides the trivial Coulomb repulsion between protons, several other repulsive interactions are known also in nuclear physics. A well-known example is the isovector particle-hole (*p-h*) interaction, which plays an important role in generating a collectivity of giant dipole resonances (GDR). The repulsive nature of the interaction is evidenced in the fact that the empirical mean GDR energy scales as $E \sim 80A^{-1/3}$ MeV, where A is the mass number of a nucleus, while a typical energy for unperturbed one-particle–one-hole (1*p*-1*h*) states is given by $E \sim 41A^{-1/3}$ MeV [18,19]. As has been argued in Ref. [20], this suggests that a similar anticorrelation to the Coulomb hole may be seen in nuclear systems as well when one considers a particle-hole pair with a proton and a neutron.

In this paper, we pursue this possibility by studying nuclei with one neutron particle and one proton hole on top of a doubly magic nucleus, such as ^{56}Co($= ^{58}$Ni $+n-p$) and ^{40}K($= ^{40}$Ca $+n-p$). We mention that the spatial anticorrelation in these nuclei was discussed long time ago by Bertsch [20]. In that paper, he employed a shell model approach to obtain the particle-hole wave functions, which were then used to compute form factors for a deuteron transfer reaction. Even though his argument is quite reasonable, the anticorrelation has not yet been demonstrated explicitly in the coordinate space. Given recent interests in dineutron correlations in neutron-rich nuclei, it would be worth revisiting this issue, especially as a correlation contrasting with the dineutron correlation.

To construct the density distribution for a particle and a hole states, we shall first obtain the ground state of the double magic nuclei in the Hartree-Fock approximation, and then linearly superpose several 1p-1h states of a neutron-proton pair. The coefficients of the superposition will be determined by diagonalizing the many-body Hamiltonian with the residual interaction. This approach is nothing but the Hartree-Fock (HF) plus Tamm-Dancoff approximation (TDA) [18,19]. Of course, one can take into account the ground state correlation of the core nuclei within the random phase approximation (RPA). However, we prefer the simpler approach of TDA, partly because the most of previous three-body model calculations for neutron-rich nuclei are based on the particle-particle TDA. We believe that a qualitative feature of the spatial distribution does not change significantly even when one employs RPA instead of TDA.

The paper is organized as follows. In Sec. II, we first detail the HF+TDA method for neutron-proton particle-hole configurations. In Sec. III, we apply the HF+TDA method to the ground and excited states of ^{56}Co and ^{40}K, and discuss the spatial correlation of the isovector particle-hole pair. We then summarize the paper in Sec. IV.

II. HARTREE-FOCK+TAMM-DANCOFF APPROXIMATION

We consider a nucleus with a neutron particle and a proton hole outside a double magic nucleus. To describe such nucleus, we first obtain the ground state of the doubly magic nucleus in the Hartree-Fock approximation. This procedure also defines the creation operators $a_p^\dagger$ for (neutron) particle states and $b_h^\dagger$ for (proton) hole states. We superpose several particle-hole pairs as

$$|\Psi\rangle = \sum_{p,h} C_{ph}|ph^{-1}\rangle \tag{1}$$

with

$$|ph^{-1}\rangle = [a_p^\dagger b_h^\dagger]|0\rangle, \tag{2}$$

where $|0\rangle$ is the ground state of the core nuclei. The coefficients C_{ph} are determined by diagonalizing a many-body Hamiltonian, whose matrix elements read [18]

$$\langle ph^{-1}|H|p'h'^{-1}\rangle = (\epsilon_p - \epsilon_h)\delta_{ph,p'h'} + \langle ph^{-1}|\bar{v}_{\text{res}}|p'h'^{-1}\rangle \tag{3}$$

$$= (\epsilon_p - \epsilon_h)\delta_{ph,p'h'} + \langle ph'|\bar{v}_{\text{res}}|hp'\rangle, \tag{4}$$

where ϵ_p and ϵ_h are single-particle energies for particle and hole states, respectively, and $\bar{v}_{\text{res}}$ is the antisymmetrized residual interaction.

Since we consider doubly magic nuclei and their vicinity, it is reasonable to assume that the nuclei we discuss in this paper are all spherical. We then introduce the notation [19]

$$a_p^\dagger = a_{jm}^\dagger, \quad b_p^\dagger = b_{jm}^\dagger = (-1)^{j+m}a_{j-m}, \tag{5}$$

where j is the total single-particle angular momentum and m is its z component. We have suppressed the isospin, the orbital angular momentum, and the radial quantum numbers to simplify the notation, but they should be understood as implicitly specified. A particle-hole state with the coupled angular momentum J and its z-component M then reads

$$|ph^{-1};JM\rangle = \sum_{m_p,m_h} \langle j_p m_p j_h m_h|JM\rangle a_{j_p m_p}^\dagger b_{j_h m_h}^\dagger|0\rangle, \tag{6}$$

$$= \sum_{m_p,m_h} (-1)^{j_h+m_h} \langle j_p m_p j_h m_h|JM\rangle$$

$$\times a_{j_p m_p}^\dagger a_{j_h -m_h}|0\rangle. \tag{7}$$

The particle-hole wave function in the coordinate space can be constructed as [21]

$$\Psi(\boldsymbol{r}_p, \boldsymbol{r}_h) = \sum_{p,h} C_{ph}\Psi_{ph}(\boldsymbol{r}_p, \boldsymbol{r}_h) \tag{8}$$

with

$$\Psi_{ph}(\boldsymbol{r}_p, \boldsymbol{r}_h) = \sum_{m_p,m_h} (-1)^{j_h+m_h} \langle j_p m_p j_h m_h|JM\rangle$$

$$\times \langle \boldsymbol{r}_p|\phi_{j_p l_p m_p}\rangle \langle \phi_{j_h l_h -m_h}|\boldsymbol{r}_h\rangle, \tag{9}$$

where $\langle \boldsymbol{r}|\phi_{jlm}\rangle = \phi_{jlm}(\boldsymbol{r})$ is a single-particle wave function with l being the orbital angular momentum. The density dis-
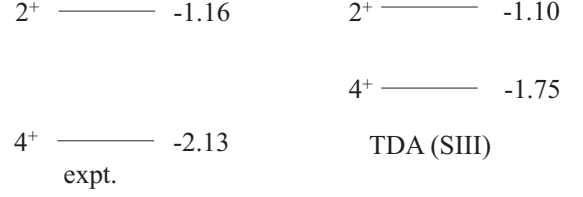

FIG. 1. The energies of the first 4^+ and 2^+ states in ^{56}Co calculated with the neutron-particle proton-hole Tamm-Dancoff approximation (TDA) with the Skyrme SIII interaction. These energies are measured from the ground state of ^{56}Ni after correcting the mass difference between a neutron and a proton.

tribution is then obtained as

$$\rho(\boldsymbol{r}_p, \boldsymbol{r}_h) = \sum_{m_s,m_{s'}} |\langle \chi_{m_s}|\Psi(\boldsymbol{r}_p, \boldsymbol{r}_h)|\chi_{m_{s'}}\rangle|^2, \tag{10}$$

where $|\chi_m\rangle$ is the spin wave function.

III. SPATIAL CORRELATION OF A NEUTRON-PROTON PARTICLE-HOLE PAIR

Let us now apply the method presented in the previous section to actual nuclei. We first discuss the ^{56}Co nucleus, which can be viewed as the doubly magic nucleus ^{56}Ni with one neutron particle and one proton hole. For this purpose, we use the Skyrme functional [22]. While we employ the full Skyrme functional for the ground state of ^{56}Ni, we use only the t_0 and t_3 terms of the residual interaction for the TDA calculations. That is, we use the isovector residual interaction given by [23]

$$\bar{v}_{\text{res}}(\boldsymbol{r}, \boldsymbol{r}') = -\left[\frac{t_0}{4}(1 + 2x_0) + \frac{t_3}{24}(1 + 2x_3)\rho(\boldsymbol{r})^\alpha\right]\boldsymbol{\tau}\boldsymbol{\tau}'$$

$$\times \delta(\boldsymbol{r} - \boldsymbol{r}'), \tag{11}$$

where $\rho(\boldsymbol{r})$ is the total density and $\boldsymbol{\tau}$ is the isospin operator. t_0, t_3, x_0, x_3, and α are parameters in the Skyrme interaction. Notice that the matrix element of the $\boldsymbol{\tau}\boldsymbol{\tau}'$ factor is $\langle pn|\boldsymbol{\tau}\cdot\boldsymbol{\tau}'|np\rangle = 2$ for a neutron-proton particle-hole pair. For simplicity, we neglect the term which is proportional to $(\boldsymbol{\sigma}\cdot\boldsymbol{\sigma}')(\boldsymbol{\tau}\cdot\boldsymbol{\tau}')$ in the residual interaction, and thus we focus only on natural parity states. The matrix elements of the residual interaction may be easily evaluated by using the helicity representation as in Ref. [2].

In this paper, we mainly employ the SIII interaction [24]. We have confirmed that the results are not qualitatively altered even if we use other parameter sets of the interaction, such as SLy4 [25]. The continuum spectrum for neutron particle states is discretized with the box boundary condition with the box size of 15 fm, and is truncated at $\epsilon_p = 40$ MeV. The calculated energies of the first natural-parity 4^+ and 2^+ states in ^{56}Co are shown in Fig. 1. These energies are given with respect to

TABLE I. The components of the wave functions in percent for the first 4^+ and 2^+ states in ^{56}Co obtained with the neutron-particle proton-hole Tamm-Dancoff approximation.

Components	4^+_1	2^+_1
$(2p_{3/2})_n(1f_{7/2})_p^{-1}$	96.4	95.5
$(2p_{1/2})_n(1f_{7/2})_p^{-1}$	2.85	–
$(1f_{5/2})_n(1f_{7/2})_p^{-1}$	0.531	3.26
$(1h_{11/2})_n(1f_{7/2})_p^{-1}$	0.00557	0.309
$(1g_{9/2})_n(1d_{5/2})_p^{-1}$	1.83×10^{-5}	0.202

the ground state of ^{56}Ni, after correcting the mass difference between a proton and a neutron. Even though our aim is not to reproduce the experimental spectrum, the agreement with the experimental data is satisfactory. The components of the wave functions for these states, that is, $|C_{ph}|^2$ in Eq. (1), are summarized in Table I. Since the single-particle levels up to $1f_{7/2}$ are fully occupied, and the lowest unoccupied level is $2p_{3/2}$, in the core nucleus ^{56}Ni, the wave functions are dominated by the $(2p_{3/2})_n(1f_{7/2})_p^{-1}$ configuration, even though there are appreciable mixtures of other components as well.

The spatial distribution for the proton hole in the two-dimensional (z, x) plane is shown in Fig. 2 for the 4^+ state in ^{56}Co with the azimuthal angular momentum component $M = 0$. To draw the figures, the location of the reference neutron particle state is fixed at $(z, x) = (3.7, 0.0)$ fm. The upper panel shows the unperturbed case with the $(1f_{7/2})_p^{-1}$ wave function. As expected, the hole wave function $(1f_{7/2})_p^{-1}$ has two symmetric peaks at the positions opposite to the center of the core nucleus. A similar feature has been known in an uncorrelated two-neutron density distribution [26]. The position of the reference neutron-particle state is in fact chosen at a place where the unperturbed hole distribution takes the maximum. The correlated hole density, in which the particle-hole repulsive interaction is active, is shown in the lower panel of Fig. 2. One can see a strong repulsive correlation, with which the component close to the reference neutron-particle state is largely hindered. This is in analogous to the Coulomb hole observed in many-electron systems, and is completely opposite to the dineutron configuration, in which the two valence neutrons stay mainly at the same side of the two-dimensional plane with a small relative distance, that is, a small correlation angle.

Figure 3 shows the spatial hole distribution for the 2^+ state in ^{56}Co. General features are quite similar to those for the 4^+ state; a strong concentration of the hole distribution at the opposite side of the reference neutron-particle with a small component of the hole distribution at the near side. A minor difference is seen in different patterns of the distributions at the center of the nucleus: almost no distribution for the 2^+ state, while an appreciable component exists in the case of the 4^+ state. Besides this, the strong repulsive correlation can be seen both in the 2^+ and the 4^+ states.

Let us next discuss the first 3^- state in ^{40}K, assuming the ^{40}Ca as a core nucleus. The ground state of ^{40}K is 4^-, and the 3^- is the lowest natural parity state. The TDA with the SIII
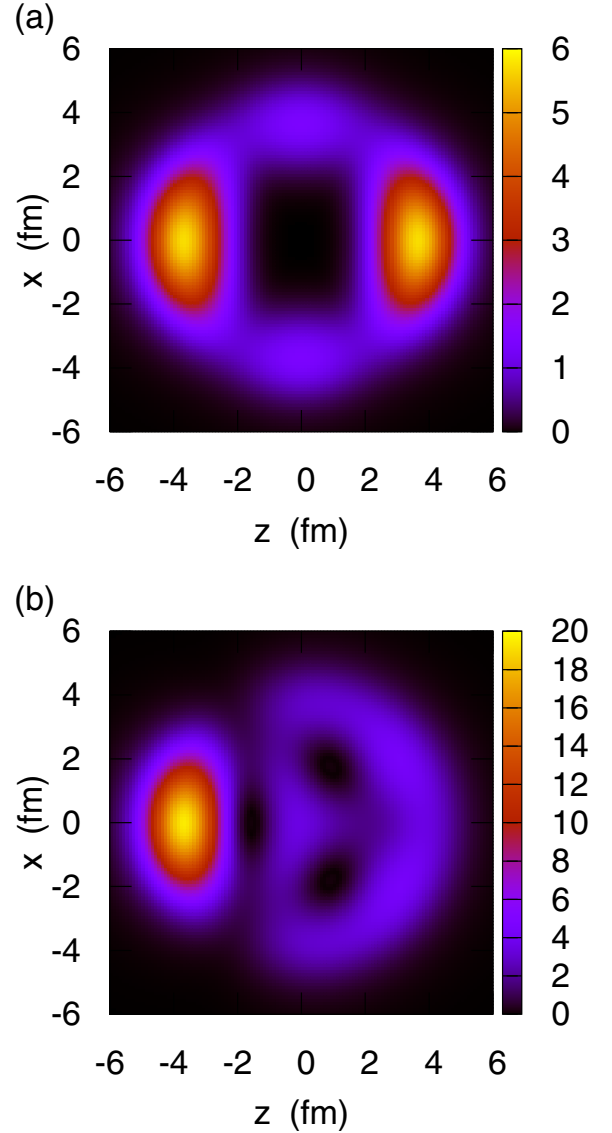

(a)

(b)

FIG. 2. The uncorrelated (upper panel) and the correlated (lower panel) proton-hole distributions in arbitrary units in the two-dimensional (z, x) plane for the 4^+ state in ^{56}Co, when the neutron-particle is located at $(z, x) = (3.7, 0.0)$ fm. The azimuthal angular momentum component is set to be $M=0$.

interaction yields the energy of the 3^- state to be $+0.052$ MeV above the ground state of ^{40}Ca after correcting the neutron-proton mass difference, whereas the empirical energy of the 3^- state is -1.28 MeV. Even though the 3^- state appears above the threshold in the present calculation, the TDA energy itself is -1.24 MeV for this state before introducing the neutron-proton mass difference, and thus the treatment of continuum state would not play a crucial role. The wave function of the 3^- state consists of 81.8% of the $(1f_{7/2})_n(1d_{3/2})_p^{-1}$ configuration, 17.9% of the $(1f_{7/2})_n(2s_{1/2})_p^{-1}$ configuration, and 0.112% of the $(1f_{7/2})_n(1d_{5/2})_p^{-1}$ configuration. The density distribution of the proton hole state is shown in Fig. 4, for the neutron-particle state fixed at $(z, x) = (2.8, 0.0)$ fm. Even though the correlation is less pronounced as compared to the
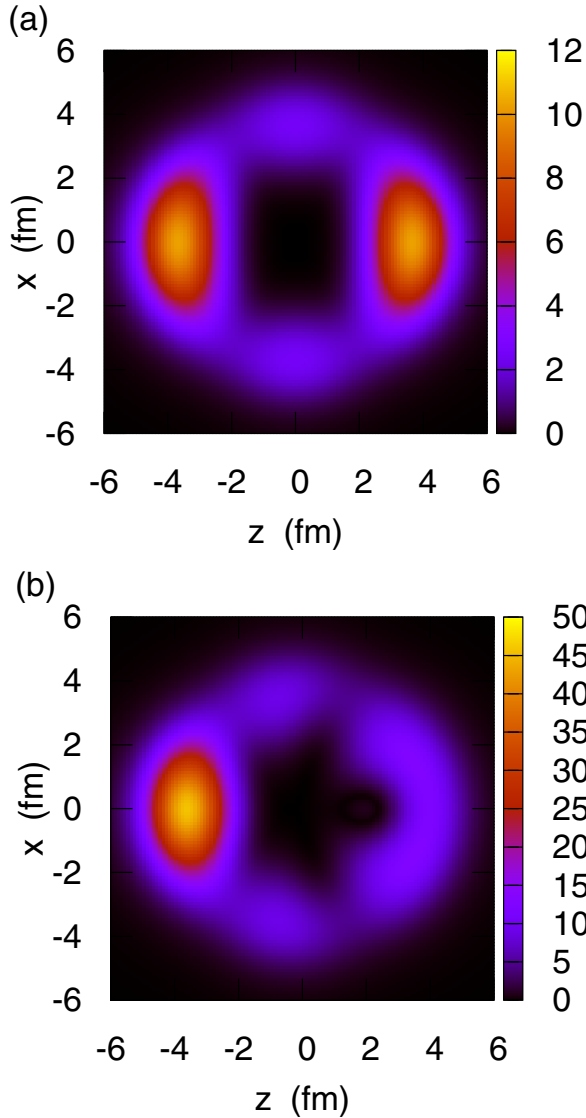
FIG. 3. The same as Fig. 2, but for the 2^+ state in ^{56}Co.

FIG. 4. The same as Fig. 2, but for the 3^- state in ^{40}K when the reference neutron-particle is fixed at $(z, x) = (2.8, 0.0)$ fm.

^{56}Co nucleus due to the *s*-wave component which has a finite value at the origin, one can see that the density in the vicinity of the reference neutron-particle is largely suppressed, reflecting the repulsive correlation between the neutron-particle and the proton-hole.

IV. SUMMARY

We have discussed the spatial correlation of an isovector particle-hole pair in ^{58}Co and ^{40}K by using the Hartree-Fock plus Tamm-Dancoff approximation with a Skyrme interaction. We have found a large concentration of the hole state distribution on the opposite side of the reference neutron-particle due to the repulsive nature of the isovector residual particle-hole interaction, as in the phenomenon of a Coulomb hole in atomic physics. This is in stark contrast to the dineutron correlation in neutron-rich nuclei, which is originated from an attractive pairing interaction between valence neutrons. This feature has been qualitatively argued in Ref. [20], but it had not yet been demonstrated in actual numerical calculations.
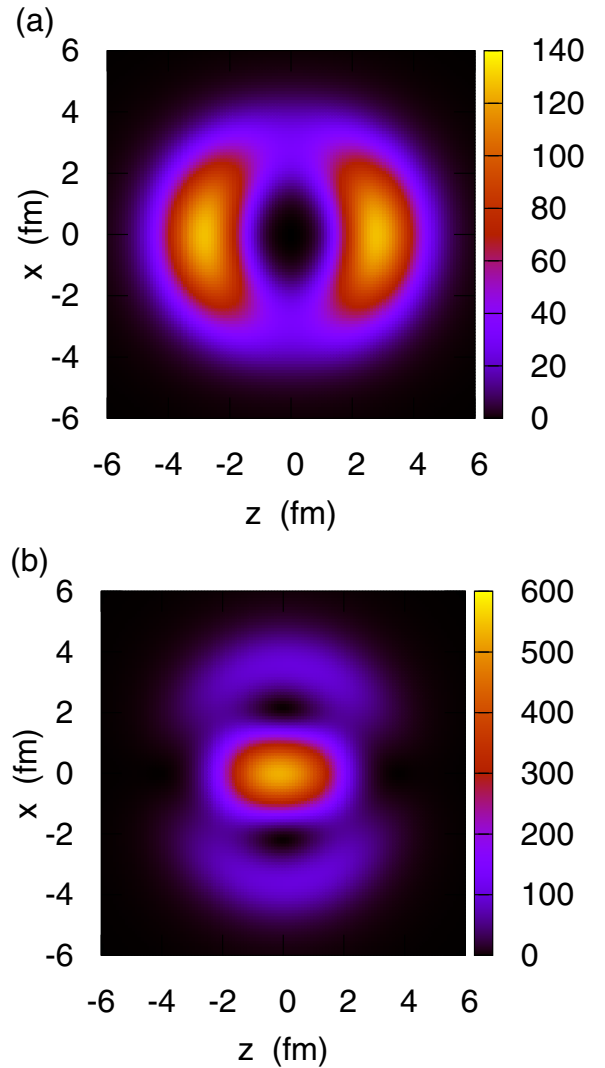
In Ref. [20], it was argued that the repulsive correlation of an isovector particle-hole pair leads to a suppression of a ground-state-to-ground-state deuteron transfer reaction, e.g., ^{54}Fe (^{3}He, p) ^{56}Co. Notice that the two proton holes in ^{54}Fe prefer the spatial configuration in which two holes are close to each other (see also the Appendix below). If one of those proton holes is filled in via a deuteron transfer, the neutron in the deuteron and the other proton hole would be located close to each other. This would correspond to an excited state of ^{56}Co, and thus, the transfer to the ground state of ^{56}Co would be largely suppressed. This scenario was confirmed theoretically based on the first order distorted-wave Born approximation (DWBA), which well reproduced the experimental data shown in Ref. [20]. Nevertheless, this scenario has yet to be confirmed with a more appropriate reaction theory for deuteron transfer reactions, which also takes into account the second order process, i.e., a sequential transfer process. It would be an

interesting future work to estimate transfer cross sections systematically with the coupled-reaction-channel method or the second order DWBA using the particle-hole wave functions obtained in this paper.

APPENDIX: HOLE-HOLE CORRELATION

Using the operator $b_{jm}^\dagger$ defined by Eq. (5) for hole states, the structure of a nucleus with two hole states from a core nucleus can be described in a similar way as a three-body model for two-particle states [2–4]. The only difference is that single-particle energies for hole states have to be multiplied by a factor of -1, as they represent removal energies of a particle from a core nucleus.

We apply this formalism to the ^{54}Fe nucleus, which can be viewed as a two proton hole state from the ^{56}Ni nucleus. To this end, we use a simple zero-range pairing interaction between the proton holes, in which the effect of Coulomb repulsion is effectively mocked up by adjusting the strength [27]. We use the Skyrme Hartree-Fock method with the SIII interaction to generate proton single-particle states in ^{56}Ni. By including all the proton hole states, the strength of the pairing interaction is adjusted to be $g = 262$ MeV fm^3 to reproduce the empirical two-proton separation energy of ^{56}Ni, $S_{2p} = 12.23$ MeV.

The resultant two-hole wave function consists of 98.5% of the $[(1f_{7/2}^{-1})^2]$ configuration, 0.748% of the $[(1d_{3/2}^{-1})^2]$ configuration, 0.433% of the $[(1d_{5/2}^{-1})^2]$ configuration, and 0.219% of the $[(2s_{1/2}^{-1})^2]$ configuration. The density distribution of the two-hole state is shown in Fig. 5. The upper panel corresponds to the density in the two-dimensional (r, θ_{12}) plane, in which $r_1 = r_2 = r$ is the distance of the hole states from the center of the nucleus and θ_{12} is the opening angle between the two holes. The weight factor of $8\pi^2 r^4 \sin\theta_{12}$ has been taken into account [4]. Notice a large two-hole probability at small opening angles around $\theta \sim 20°$. The lower panel, on the other
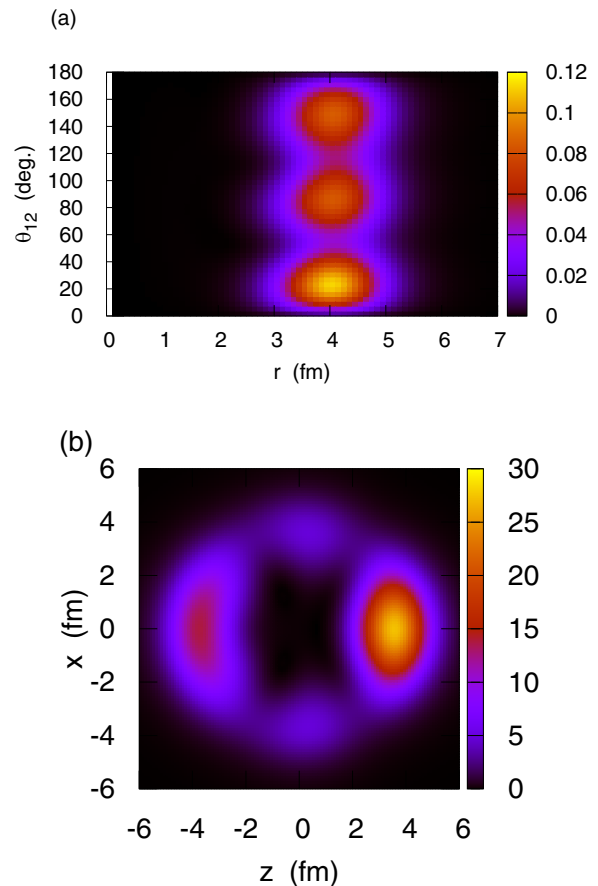

FIG. 5. The distribution of the two-hole configuration in ^{56}Ni obtained with the hole-hole Tamm-Dancoff approximation. The upper panel shows the density distribution for the two hole states obtained by setting $r_1 = r_2 = r$. This is plotted as a function of r and the opening angle, θ_{12}. The weight factor $8\pi^2 r^4 \sin\theta_{12}$ has been multiplied. The lower panel shows the density of the second hole in arbitrary units when the first hole is fixed at $(z, x) = (3.7, 0.0)$ fm.

hand, shows the distribution of the second hole when the first hole is fixed at $(z, x) = (3.7, 0.0)$ fm. One can clearly see an enhancement of the density distribution when the two hole states are located at similar places. This is basically the same phenomenon as the dineutron correlation discussed in Ref. [4].

[1] J. Dobaczewski, W. Nazarewicz, T. R. Werner, J. F. Berger, C. R. Chinn, and J. Dechargé, Phys. Rev. C **53**, 2809 (1996).

[2] G. F. Bertsch and H. Esbensen, Ann. Phys. (NY) **209**, 327 (1991).

[3] H. Esbensen, G. F. Bertsch, and K. Hencken, Phys. Rev. C **56**, 3054 (1997).

[4] K. Hagino and H. Sagawa, Phys. Rev. C **72**, 044321 (2005).

[5] F. Barranco, P. F. Bortignon, R. A. Broglia, G. Colo, and E. Vigezzi, Eur. Phys. J. A **11**, 385 (2001).

[6] K. Hagino, I. Tanihata, and H. Sagawa, in *100 Years of Subatomic Physics*, edited by E. M. Henley and S. D. Ellis (World Scientific, Singapore, 2013), p. 231.

[7] K. Hagino, H. Sagawa, J. Carbonell, and P. Schuck, Phys. Rev. Lett. **99**, 022506 (2007).

[8] M. Matsuo, K. Mizuyama, and Y. Serizawa, Phys. Rev. C **71**, 064326 (2005).

[9] N. Pillet, N. Sandulescu, and P. Schuck, Phys. Rev. C **76**, 024310 (2007).

[10] M. V. Zhukov, B. V. Danilin, D. V. Fedorov, J. M. Bang, I. J. Thompson, and J. S. Vaagen, Phys. Rep. **231**, 151 (1993).

[11] T. Nakamura *et al.*, Phys. Rev. Lett. **96**, 252502 (2006).

[12] T. Aumann *et al.*, Phys. Rev. C **59**, 1252 (1999).

[13] Y. Kubota *et al.*, Phys. Rev. Lett. **125**, 252501 (2020).

[14] K. J. Cook *et al.*, Phys. Rev. Lett. **124**, 212503 (2020).

[15] G. Munschy and P. Pluvinage, Rev. Mod. Phys. **35**, 494 (1963).

[16] P. Rehmus and R. S. Berry, Chem. Phys. **38**, 257 (1979).

[17] R. J. Boyd and M. C. Yee, J. Chem. Phys. **77**, 3578 (1982).

[18] P. Ring and P. Schuck, *The Nuclear Many Body Problem* (Springer-Verlag, New York, 1980).

[19] D. J. Rowe, *Nuclear Collective Motions* (World Scientific, Singapore, 2010).

[20] G. F. Bertsch, Phys. Lett. B **25**, 62 (1967).

[21] G. F. Bertsch, R. A. Broglia, and C. Riedel, Nucl. Phys. A **91**, 123 (1967).

[22] D. Vautherin and D. M. Brink, Phys. Rev. C **5**, 626 (1972).

[23] I. Hamamoto and H. Sagawa, Phys. Rev. C **60**, 064314 (1999).

[24] M. Beiner, H. Flocard, Nguyen Van Giai, and P. Quentin, Nucl. Phys. A **238**, 29 (1975).

[25] E. Chabanat, P. Bonche, P. Haensel, J. Meyer, and R. Schaeffer, Nucl. Phys. A **635**, 231 (1998).

[26] K. Hagino, H. Sagawa, and P. Schuck, J. Phys. G: Nucl. Part. Phys. **37**, 064040 (2010).

[27] T. Oishi, K. Hagino, and H. Sagawa, Phys. Rev. C **82**, 024315 (2010).